New Transceiver Scheme for OFDM-Based Broadband Power Line Communications

EMAD S. HASSAN[1, 2]

[1]Dept. of Electrical Engineering
Jazan University
Jazan
KSA.
eshassan@jazanu.edu.sa

[2]Dept. of Electronics and Electrical Communications
Menoufia University
Faculty of Electronic Engineering, Menouf, 32952
EGYPT
eng_emadash@yahoo.com

Abstract: - Power line communications (PLC), thanks to the widespread availability of power line infrastructure, is considered as a low-cost alternative for data transmission. Power lines, however, remain hostile environments for communication signal propagation. In this paper, we propose a new transceiver scheme for orthogonal frequency division multiplexing (OFDM)-based broadband power line communications (BPLC) that implements discrete cosine transform (DCT) and continuous phase modulation (CPM). The proposed transceiver combines the advantages of superior bit error rate (BER) performance of DCT-OFDM, in addition to exploiting the channel frequency diversity and the power efficiency of CPM. Then, the paper presents a chaotic interleaving scheme for the proposed transceiver to further improve the BER performance of BPLC. Moreover, it increases the security of BPLC. The BER performance of BPLC with conventional OFDM and with proposed transceiver scheme (DCT-CPM-OFDM) is evaluated by computer simulations. The obtained results show that, the proposed transceiver scheme is robust to channel impairments while maintaining superior BER performance especially when using chaotic interleaving. As a real application of the proposed transceiver, we check the transmissions of images over a real PL channel. Images with high peak signal to noise ratio (PSNR) are received and the proposed transceiver is shown to have a good performance over PL channels.

Key-Words: - BPLC, OFDM, DCT, CPM, Chaotic interleaving, Equalization.

1 Introduction

In the past several years, the demand for broadband multimedia applications has significantly increased and continues to grow at a rapid pace. A variety of technologies are currently in use for broadband connectivity to and within homes and offices. Among those communication technologies, power line communications (PLC) is receiving a huge amount of research interest and presents a very attractive multimedia connectivity solution to the last-mile problem [1-3]. Broadband PLC (BPLC) exploits already-existing electrical networks to deliver high-speed broadband communications [3-4]. In addition to solving the last-mile connectivity issue, PLC uses the in-building electrical wiring as a local area network providing high-speed networking that includes broadband Internet access, voice over IP and home entertainment services to virtually every power socket in residential or business premises. The driving advantage of PLC is that it uses an infrastructure that is much more ubiquitous than any other wired infrastructure, hence does not require new wiring. PLC offers a competitive and cost-effective alternative for Internet access and LAN applications [1-5].

Despite the PLC advantages, this technology conveys communication signals through a medium that was never designed for telecommunication functions. Power lines differ significantly in their structure and physical characteristics from usual communication mediums such as coaxial cables and optical fiber [6-8]. PL cables suffer from considerable frequency-dependant attenuation that increases with high frequencies and can be severe for long-distance communications. Moreover, impedance mismatching is commonly present in PL networks causing enormous reflections of the signal, giving rise to multipath fading [6]. Another persistent impairment for PLC systems is the noise generated by internal and external sources that are either connected or in close proximity to the PLC transmission medium. The noise at any power outlet is the sum of noises produced by different appliances connected to the line plus the background noise on the line [7-8].

Due to the presence of undesirable characteristics of PL channel, it is crucial for high-speed PLC to

select a modulation technique that can stand against such peculiarities. A number of modulation techniques, including single-carrier, multi-carrier and spread spectrum are of interest for PLC engineers and researchers [1], [9]. Among those, orthogonal frequency division multiplexing (OFDM) stands as an excellent candidate for PLC [10-12]. OFDM is an attractive multicarrier transmission technique for wideband communications because it effectively transforms the frequency selective fading channel into a flat fading channel. Hence, OFDM provides greater immunity to multipath fading and impulsive noise, and eliminates the need for complicated equalizers [12-13]. OFDM offers robustness as well as simple implementation which make this technique a favored candidate for PLC.

Several solutions have been proposed as alternatives to conventional discrete Fourier transform (DFT)-based OFDM systems, such as the use of filter banks [14] or discrete trigonometric transforms such as discrete cosine transform (DCT) [15]–[18]. The excellent energy compaction property of the DCT makes most of the signal energy concentrated in the first few samples, leaving the rest of samples close to zero. If the DCT is used prior to data transmission through PL, it is expected that the inter-symbol interference (ISI) resulting from those small amplitude samples will be very small, leading to a lower bit error rate (BER) than the case with the DFT. Recently, much attention has been given to the DCT based OFDM due to its advantages over the DFT-based OFDM [16].

This paper proposes a new transceiver scheme for OFDM-based BPLC that implements DCT and continuous phase modulation (CPM). The CPM approach [13, 19-20] is attractive for wireless communications, because of the constant envelope of the generated signals, which is needed for power efficient transmitters, and its ability to exploit the diversity of the multipath channel, which is needed to improve the BER performance. In the CPM-OFDM system, the OFDM signal is used to phase-modulate the carrier. This system shares many of the same functional blocks with the conventional OFDM system. This makes the existing OFDM systems capable of providing an additional CPM-OFDM mode, easily. Therefore, DCT- based OFDM can be fruitfully combined with CPM to get the advantages of superior BER performance of DCT-OFDM, in addition to exploiting the channel frequency diversity and the power efficiency of CPM.

Under harsh channel conditions of PL channels, the reliability of BPLC can be further improved by the utilization of interleaving. Interleaving is a process to rearrange the samples of the transmitted signal so as to spread bursts of errors over multiple code words [21]. This paper also presents a chaotic interleaving scheme [21-23] for the proposed transceiver to further improve its BER performance and to combat the bursty nature of the impulsive noise present in PL channels. Chaotic interleaving is used to generate permuted versions from the sample sequences to be transmitted, with low correlation among their samples, and hence a better BER performance can be achieved. Several experiments are carried out to test the BER performance of BPLC with conventional OFDM and with proposed transceiver scheme (DCT-CPM-OFDM). The superior performance of the proposed transceiver scheme is proved.

The rest of this paper is organized as follows. Section 2 presents the proposed CPM based-DCT-OFDM system model. The frequency-domain equalizer design is presented in section 3. The proposed chaotic interleaving mechanism is explained in section 4. Section 5 presents the spectral efficiency and multipath diversity of CPM signals. Section 6 introduces the simulation results. Finally, Section 7 gives the concluding remarks.

2 CPM-based DCT-OFDM System Model

The block diagram of the CPM-based DCT-OFDM system is shown in Fig. 1. Let $X(k)$ denote the M-ary quadrature amplitude modulation (QAM) data symbols. During each T-second block interval, an N_{DCT} points IDCT is used to give the block of time samples $x(n)$ corresponding to $X(k)$. After that, the generated OFDM sequence, $x(n)$, passes through a phase modulator (PM) to get the constant envelope sequence $s(n) = \exp(jCx(n))$, where C is a scaling constant. After the PM, a cyclic prefix (CP) is added at the beginning of each data block to help mitigating the inter-block interference (IBI), which is assumed to have a longer length than the channel impulse response.

The continuous-time CPM-OFDM signal $s(t)$ is then generated at the output of the digital-to-analog (D/A) converter. This signal can be expressed as follows [12], [19]:

$$s(t) = Ae^{j\phi(t)} = Ae^{j[2\pi hx(t)+\theta]}, \qquad T_g \le t < T \qquad (1)$$

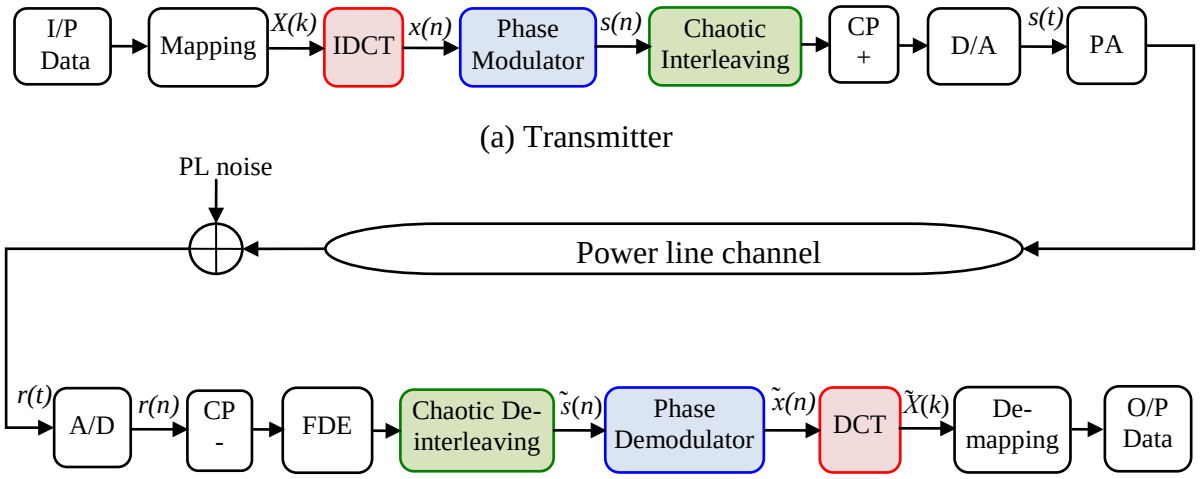

Figure 1: Block diagram of the CPM-OFDM system.

where A is the signal amplitude, h is the modulation index, θ is an arbitrary phase offset used to achieve CPM [12], T_g is the guard period, T is the block period, and $x(t)$ is a real-valued OFDM message signal comprised of K subcarriers and given as:

$$x(t) = C_n \sum_{k=0}^{K-1} I_k \beta_k \cos\left(\frac{\pi k(2t+1)}{2N}\right) \quad (2)$$

where C_n is a normalization constant used to normalize the variance of the message signal (i.e., $\sigma^2_x = 1$), and consequently the variance of the phase signal, $\sigma^2_\varphi = (2\pi h)^2$. This requirement is achieved by setting C_n as follows [12]:

$$C_n = \sqrt{\frac{2}{K\sigma_I^2}} \quad (3)$$

where σ^2_I is the variance of the data symbols. The assumption that the data is independent and identically distributed leads to:

$$\sigma_I^2 = E\left\{ |X(k)|^2 \right\} = \frac{1}{M}\sum_{l=1}^{M}(2l-1-M)^2 = \frac{M^2-1}{3} \quad (4)$$

where M is the number of constellation points.
In Eq. (2), I_k are the real-valued data symbols:

$$I_k = \begin{cases} \Re\{X(k)\}, & k \le K/2 \\ -\Im\{X(k-K/2)\}, & k > K/2 \end{cases} \quad (5)$$

where $\Re\{X(k)\}$, $\Im\{X(k)\}$ are the real and the imaginary part of $\{X(k)\}$, respectively and $\beta(k)$ can be expressed as follows [18]:

$$\beta_k = \begin{cases} \frac{1}{\sqrt{2}} & k = 0 \\ 1 & k = 1,2,\ldots\ldots,K-1 \end{cases} \quad (6)$$

2.1 Power Line Channel Model

Then, the transmitted signal $s(t)$ passes through the multipath channel. Power line networks differ significantly in topology, structure, and physical properties from conventional communication channels such as twisted pair, coaxial, or fiber-optic cables [5, 7]. Because they were not specifically designed for data transmission, power lines provide a harsh environment for higher frequency communication signals. The most influential properties of this hostile medium in the performance of high speed communications are signal distortion due to frequency-dependant cable losses, multi-path propagation and noise [7]. The PL channel transfer function can be expressed as [5, 7]:

$$H(f) = \sum_{l=0}^{L-1} c_l . e^{-\left(a_0 + a_1 f^k\right) d_l} . e^{-j2\pi f\left(d_l / v_p\right)} \quad (7)$$

where L is the number of multi-paths, c_l and d_l are the weighting factor and length of the lth path respectively. In Eq. (7), the first exponential presents attenuation in the PLC channel, whereas the second exponential, with the propagation speed v_p, describes the echo scenario. Frequency-dependant attenuation is modeled by the parameters a_0, a_1 and k. The attenuation parameters for a 4-path model and a 15-path model were obtained using physical measurements and summarized in [5].

2.2 Noise Model

The noise present in power lines is often categorized into classes. According to [6], there are five types of noise: colored background noise, narrowband noise, periodic impulsive noise asynchronous to the mains frequency, periodic impulsive noise synchronous to the mains frequency and asynchronous impulsive noise. The first three noise types listed above usually remain stationary over long periods of time and can be summarized as background noise (w_k). The last two types have a time-varying nature and can be summarized as impulsive noise (i_k).

The transmitted signal $s(t)$ passes through a PL channel expressed by the channel transfer function $H(f)$ given in Eq. (7). Then, the different types of noise are added to $s(t)$ before arriving at the receiver. The continuous-time received signal $r(t)$ is expressed as:

$$r(t) = \sum_{l=0}^{L-1} h(l)s(t-\tau_l) + w(t) + i(t) \tag{8}$$

where h is the PL channel impulse response which is the inverse Fourier transform of the transfer function defined in Eq. (7).

To analyze the effect of noise in OFDM-based PLC systems, the background noise $w(t)$ is modeled as an AWGN with zero mean and variance σ^2_w [12]. The impulsive noise $i(t)$ is modeled using the Poisson-Gaussian noise model [24-25]. According to this model, impulsive noise is given by the following:

$$i(t) = p(t)g(t) \tag{9}$$

where p is the Poisson Process which corresponds to the arrival of impulsive noise, and g is white Gaussian process with zero mean and variance σ^2_g.

The output of the analog-to-digital (A/D) converter is sampled at a sampling rate $f_s = JK/T$ sample/sec. The n^{th} sample of the received signal $r(t)$ is given by:

$$r(n) = \sum_{i=0}^{LJ-1} h(i)s(n-i) + w(n) + i(n) \tag{10}$$

where J denotes the oversampling factor. After the A/D, the CP samples are discarded and the remaining samples are equalized with frequency-domain equalization (FDE) process.

3 Frequency-domain Equalizer Design

In order to mitigate multipath effects and enhance the performance of BPLC based systems, we must apply FDE. As shown in Fig. 1, the received signals are equalized in the frequency domain. Let $W(m)$, (m = 0, 1,…,N_{DFT} -1), denotes the equalizer coefficients for the *mth* subcarrier, the time domain equalized signal $\tilde{s}_I(i)$, which is the soft estimate of $s_I(i)$, can be expressed as follows:

$$\tilde{s}_I(i) = \frac{1}{N_{DFT}} \sum_{m=0}^{N_{DFT}-1} W(m)R_I(m)e^{j2\pi mi/N_{DFT}} \tag{11}$$

The equalizer coefficients $W(m)$ are selected to minimize the mean squared error between the equalized signal $\tilde{s}_I(n)$ and the original signal $s_I(n)$. The equalizer coefficients are computed according to a certain optimization rule leading to several types of equalizers, such as the zero forcing (ZF) and the minimum mean square error (MMSE) equalizers [21-23]. In this paper we consider the MMSE, for this type, the equalizer coefficients $W(m)$ is given as [21],

$$W(m) = \frac{H^*(m)}{|H(m)|^2 + (E_b/N_0)^{-1}} \tag{12}$$

The de-interleaving is then applied to the equalized samples. Afterwards, a phase demodulation step is applied to recover the data as explained in the next sections.

4 Chaotic Interleaving Mechanism

Error correction codes are usually used to protect signals through transmission over channels. Most of the error correction codes are designed to correct random channel errors. However, channel errors caused by PL channels are bursty in nature. Interleaving is a process to rearrange the samples of the transmitted signal so as to spread bursts of errors over multiple code words.

As explained in section 2, power lines provide a harsh environment for higher frequency communication signals, because they were not specifically designed for data transmission. As a result, there is a need for advanced interleaver to reduce the channel effects. The 2-D chaotic Baker map in its discretized version is a good candidate for this purpose [26]. Due to the inherent strong randomization ability of these maps, they can be efficiently used for data interleaving.

After PM, the signal samples can be arranged into a 2-D format then randomized using the chaotic Baker map. The chaotic interleaver generates permuted sequences with lower correlation between their samples and adds a degree of encryption to the transmitted signal [21-23].

The discretized Baker map is an efficient tool to randomize the items in a square matrix. Let $B(n_1,\ldots,n_k)$, denote the discretized map, where the vector, $[n_1, \ldots, n_k]$, represents the secret key, S_{key}. Defining N as the number of data items in one row, the secret key is chosen such that each integer n_i divides N, and $n_1 + \ldots + n_k = N$.

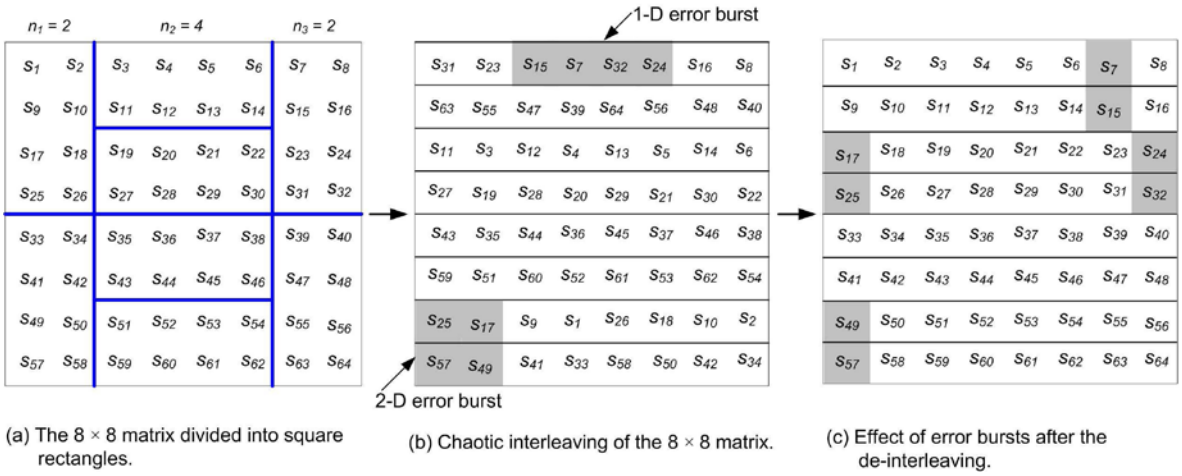

Figure 2: Chaotic interleaving of an 8 × 8 matrix.

Let $N_i = n_1 + \ldots + n_i$. The data item at the indices (q, z), is moved to the indices [21], [23]:

$$B_{(n_1,\ldots,n_k)}(q,z) = \begin{pmatrix} \frac{N}{n_i}(q - N_i) + z \bmod\left(\frac{N}{n_i}\right), \\ \frac{n_i}{N}\left(z - z \bmod\left(\frac{N}{n_i}\right)\right) + N_i \end{pmatrix} \quad (13)$$

where $N_i \leq q < N_i + n_i$, and $0 \leq z < N$.

In steps, the chaotic permutation is performed as follows:

1) An $N \times N$ square matrix is divided into k rectangles of width n_i and number of elements N.
2) The elements in each rectangle are rearranged to a row in the permuted rectangle. Rectangles are taken from left to right beginning with upper rectangles then lower ones.
3) Inside each rectangle, the scan begins from the bottom left corner towards upper elements.

Figure 2 shows an example for the chaotic interleaving of an (8 × 8) square matrix (i.e. $N = 8$). The secret key, $S_{key} = [n_1, n_2, n_3] = [2, 4, 2]$. Note that, the chaotic interleaving mechanism has a better treatment to both 1-D and 2-D bursts of errors than the block interleaving. Errors are better distributed to samples after de-interleaving in the proposed chaotic interleaving mechanism. As a result, a better BER performance can be achieved with the proposed interleaving mechanism. Moreover, it adds a degree of security to the communication system. At the receiver of the proposed systems with chaotic interleaving, the received signal is then passed through an A/D converter, then the CP is discarded and the remaining samples are equalized as will be discussed in the next section to study the effect of the proposed chaotic interleaving scheme on the overall system performance.

5 Spectral Efficiency and Multipath Diversity of CPM Signals

The spectral efficiency is an important quality metric for a modulation format, since it quantifies how many information bits per second can be loaded per unity of the available bandwidth. To evaluate the spectral efficiency of a signal, its bandwidth needs to be estimated. Using Taylor expansion, the CPM signal described in Eq. (1), when $\theta = 0$, can be rewritten as:

$$s(t) = Ae^{j2\pi hx(t)} = A\sum_{n=0}^{\infty}\left[\frac{(j2\pi h)^n}{n!}\right]x^n(t) \quad (14)$$

$$= A\left[1 + j2\pi hx(t) - \frac{(2\pi h)^2}{2!}x^2(t) - j\frac{(2\pi h)^3}{3!}x^3(t) + \ldots\right]$$

The subcarriers are centered at the frequencies $\pm i/T$ Hz, $i = 1, 2, \ldots, K/2$. The effective double-side bandwidth of the message signal, $x(t)$, is defined as $W = K/T$ Hz. According to Eq.(17), the bandwidth of $s(t)$ is at least W, if the first two terms only of the summation are considered. Depending on the modulation index value, the effective bandwidth can be greater than W. A useful bandwidth expression for the CPM signal is the root-mean-square (RMS) bandwidth [30]:

$$\text{BW} = \max(2\pi h, 1)W \quad \text{Hz} \quad (15)$$

As shown in Eq. (15), the signal bandwidth grows with $2\pi h$, which in turn reduces the bandwidth efficiency. Since the bit rate is $R = K(\log_2 M)/T$ bps, the spectral efficiency of the CPM signal, η, can be expressed as:

$$\eta = \frac{R}{\text{BW}} = \frac{\log_2 M}{\max(2\pi h, 1)} \quad \text{bps/Hz} \quad (19)$$

The spectral efficiency of a CPM signal is controlled by two parameters, M and $2\pi h$. On the other hand, the spectral efficiency of an OFDM signal is $\log_2 M$, which depends only on M.

The Taylor expansion given in Eq. (14) reveals how a CPM signal exploits the frequency diversity in the channel for a large modulation index. This is not necessary the case, however. For a small modulation index, only the first two terms in Eq. (14) contribute:

$$s(t) \approx A\left[1 + j2\pi h m(t)\right] \quad (20)$$

In this case, the CPM signal does not have the frequency spreading given by the higher-order terms. Therefore, the CPM signal does not have the ability to exploit the frequency diversity of the channel [21].

6 Numerical Results and Discussion

In this section, simulation experiments are carried out to demonstrate the effectiveness of the proposed transceiver. Two different channel models are utilized in the simulation experiments conducted in this paper [5]. Channel A: 4-path channel with parameters given in Table 1 and Channel B: 15-path channel with parameters given in Table 2 [5]. The arrival of impulsive noise is assumed to follow a Poisson distribution as described in Eq. (9) while the background noise is assumed to be AWGN. The 4-ary (M = 4) QAM is used in the simulations. Each block contains K = 128 subcarrier.

Table 1: PL channel A parameters.

Attenuation parameters					
$k = 1$ $a_0 = 0$ $a_1 = 7.8 \times 10^{-10}$ m/s					
Path-parameters					
l	c_l	$d_l(m)$	l	c_l	$d_l(m)$
1	0.64	200	**3**	-0.15	244.8
2	0.38	222.4	**4**	0.05	267

6.1CPM-based DCT-OFDM versus Conventional CPM-OFDM Results

Figure 3 shows the effect of the modulation index on the performance of the CPM-based DCT-OFDM system, at a fixed signal-to-noise ratio (SNR) = 20 dB, for both single path and multi-path PL channel (A and B) cases. It is clear from this figure that, the BER of CPM-based DCT-OFDM system decreases with the increase of the modulation index, $2\pi h$ and reaches its optimum value at $2\pi h$ = 1.3 for both channels A and B. It is clear also that, the performance of CPM-based DCT-OFDM system over a multi-path channel is better than its performance over a single path channel for $2\pi h >$ 0.4, which clarifies that the proposed CPM-based DCT-OFDM system exploits the multi-path diversity of the channel for large modulation indices and for large number of channel paths as in channel B. For small modulation indices between 0 and 0.4, the performance over a single path channel constitutes a lower bound for the performance over a multi-path channel as indicated by figure 4.

Table 2: PL channel B parameters.

Attenuation parameters					
$k = 1$ $a_0 = 0$ $a_1 = 2.5 \times 10^{-9}$ m/s					
Path-parameters					
l	c_l	$d_l(m)$	l	c_l	$d_l(m)$
1	0.029	90	**9**	0.071	411
2	0.043	102	**10**	-0.035	490
3	0.103	113	**11**	0.065	567
4	-0.058	143	**12**	-0.055	740
5	-0.045	148	**13**	0.042	960
6	-0.040	200	**14**	-0.059	1130
7	0.038	260	**15**	0.049	1250
8	-0.038	322			

From the above discussion it is clear that, there is a trade-off between BER performance which is improved by increasing the modulation index, and spectral efficiency which is improved by decreasing the modulation index. Based on the performance shown in figures 3 and 4, and the spectral efficiency given by Eq. (19), it can be deduced that a moderate modulation index leads to an efficient utilization of the channel frequency diversity, while maintaining acceptable spectral efficiency. In the following results, we will use $2\pi h$ = 1 to make a good trade-off between the BER performance and the spectral efficiency.

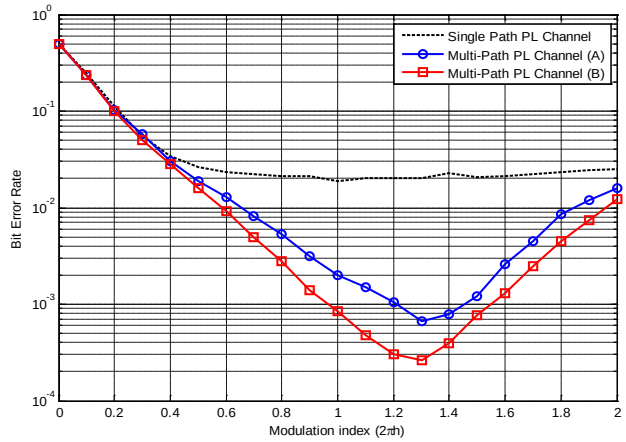

Figure 3: Impact of the modulation index on the performance of CPM-based DCT-OFDM system for both single path and multi-path channel cases at SNR = 20 dB.

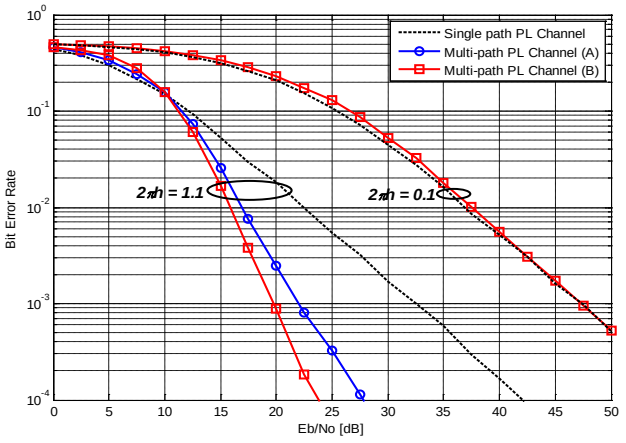

Figure 4: BER performance of CPM-based DCT-OFDM system over single path and multi-path PL channels, using the channel models A and B and an MMSE equalizer.

Figure 5 shows the performance comparison between the proposed CPM-based DCT-OFDM system and the conventional CPM-OFDM system described in [12] in terms of modulation index using MMSE equalizer. It is clear that, the proposed system outperforms the conventional CPM-OFDM system at a relatively small modulation index. So we can say that, the DCT improves the spectral efficiency when used with CPM-OFDM system.

Table 3 shows the improvement percentage in spectral efficiency of the proposed CPM-based DCT-OFDM system over the conventional CPM-OFDM system [12]. For example, at BER of 3.4×10^{-4} and $M = 4$, the proposed system, needs $2\pi h = 1.15$ and according to Eq. (19), the spectral efficiency will be $\eta = 1.74$ *bps*. On the other hand, the conventional CPM-OFDM system needs $2\pi h = 1.3$, *i.e.* $\eta = 1.53$ *bps* which means that, the proposed CPM-based DCT-OFDM system can achieves about 13.7% improvements in spectral efficiency when compared to the conventional CPM-OFDM system.

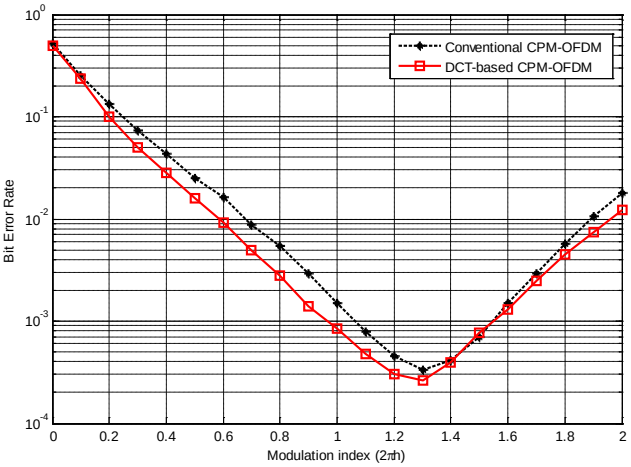

Figure 5: BER performance of the conventional CPM-OFDM and the proposed CPM-based DCT-OFDM systems in terms of $2\pi h$ at SNR = 20 dB.

Figure 6 shows a comparison between conventional OFDM system, conventional CPM-based DFT-OFDM system and the proposed CPM-based DCT-OFDM system. The AWGN channel is included as a reference channel. It is clear from this figure that, at a BER of 10^{-3}, the proposed system outperforms the conventional CPM-based DFT-OFDM system and the conventional OFDM system by 2.4 dB and 14.3 dB, respectively. The figure reveals that the proposed CPM-based DCT-OFDM system solves the problems of conventional OFDM system at higher SNRs.

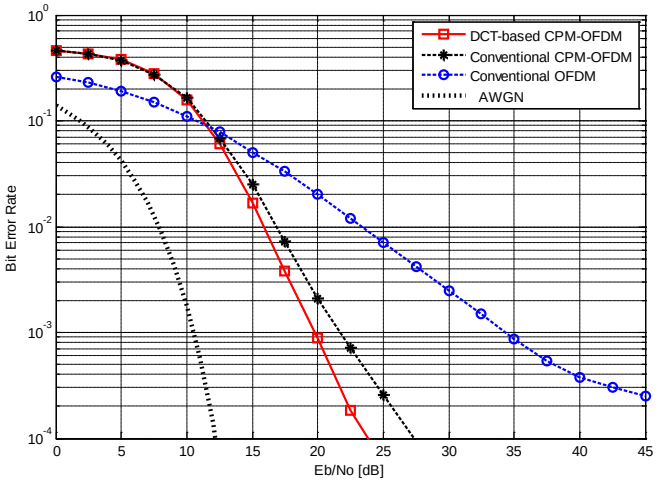

Figure 6: BER performance of the conventional OFDM system, the conventional CPM-OFDM system, and the proposed system using channel model B and an MMSE equalizer.

Table 3: Improvement percentage in spectral efficiency for the conventional CPM-OFDM system and the proposed system.

BER	Conventional CPM-OFDM	Proposed CPM-based DCT-OFDM	% improvement
8.5×10^{-4}	$\eta = 1.818$ *bps* $(2\pi h = 1.1)$	$\eta = 2$ *bps* $(2\pi h = 1)$	10 %
3.4×10^{-4}	$\eta = 1.53$ *bps* $(2\pi h = 1.3)$	$\eta = 1.74$ *bps* $(2\pi h = 1.15)$	13.7 %

6.2 Chaotic interleaving Results

Figure 7 shows a performance comparison between the CPM-based DCT-OFDM with and without chaotic interleaving in terms of the modulation index in the multi-path channel B case. It is clear that, the proposed CPM-based DCT-OFDM system with chaotic interleaving outperforms the CPM-based DCT-OFDM system without interleaving at relatively small modulation index values. This means that the proposed chaotic interleaving scheme further improves the spectral efficiency of the CPM-based DCT-OFDM system.

Table 4 shows the percentage of improvement in spectral efficiency of the proposed CPM-based DCT-OFDM system with and without chaotic interleaving when $M = 4$. For example, at a BER of 2.2×10^{-4}, the CPM-based DCT-OFDM system without interleaving needs $2\pi h = 1.3$, and hence the spectral efficiency will be $\eta = 1.53$ bps. On the other hand, the proposed CPM-SC-FDE system with chaotic interleaving needs $2\pi h = 1$, *i.e.* $\eta = 2$ bps, which means that the chaotic interleaving achieves an improvement in spectral efficiency of about 30.7 %, when it used with the CPM-based DCT-OFDM system. We can go to a conclusion that the proposed CPM-based DCT-OFDM system with chaotic interleaving achieves a trade-off between the performance and the spectral efficiency, which is one of the most serious problems in CPM based systems.

Figure 8 shows the BER performance of the proposed CPM-based DCT-OFDM system with and without chaotic interleaving MMSE equalizer and channel model B. The results show that, the chaotic interleaving further improves the BER performance of the proposed system. For example, at a BER = 10^{-3}, the proposed system with chaotic interleaving outperforms its performance without interleaving by about 2.5 dB.

6.3 Real PLC System Results

To illustrate the performance of the proposed transceiver, cameraman image is transmitted through a real power-line channel. The experimental environment is shown in Fig. 9. The TMDSPLCKIT-V3 [27] is used as the transmitter

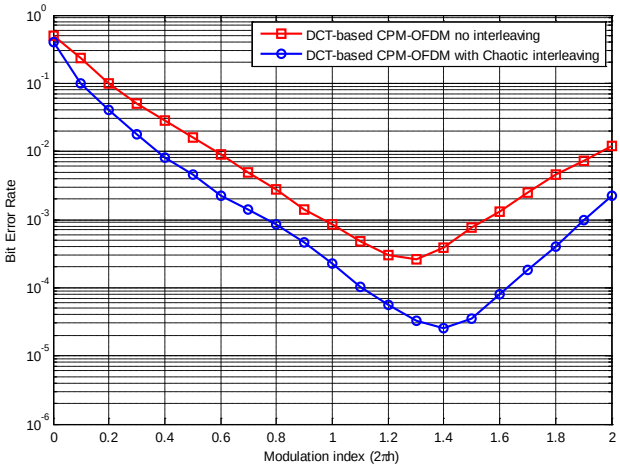

Figure 7: BER performance of the CPM-based DCT-OFDM system with and without chaotic interleaving vs. the modulation index at an SNR = 20 dB.

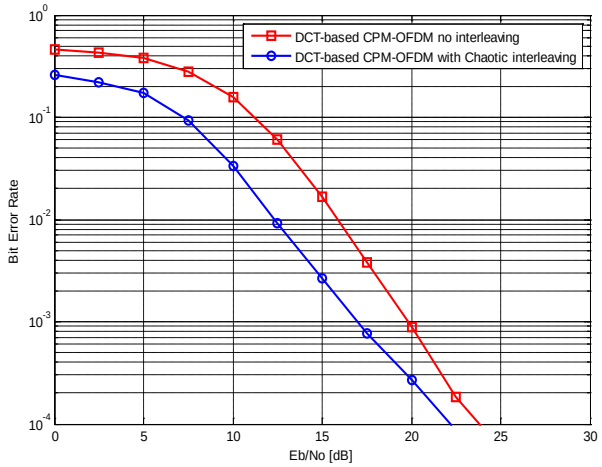

Figure 8: BER performance of the CPM-based DCT-OFDM system with and without chaotic interleaving using channel model B and an MMSE equalizer.

and the TMDSIACLEDCOMKIT [28] is used as the receiver. The main features of these kits are as follows; they use conventional OFDM for data transmission using 64 sub-carriers, they use convolutional encoder and Viterbi decoder and bit interleaving.

Table 4: Improvement percentage in spectral efficiency for the CPM-based DCT-OFDM system with and without chaotic interleaving.

BER	CPM-SC-FDE (no interleaving)	CPM-SC-FDE (with chaotic interleaving)	% improvement
3×10^{-4}	$\eta = 1.67$ *bps* $(2\pi h = 1.2)$	$\eta = 2$ *bps* $(2\pi h = 0.96)$	19.7 %
2.2×10^{-4}	$\eta = 1.53$ *bps* $(2\pi h = 1.3)$	$\eta = 2$ *bps* $(2\pi h = 1)$	30.7 %

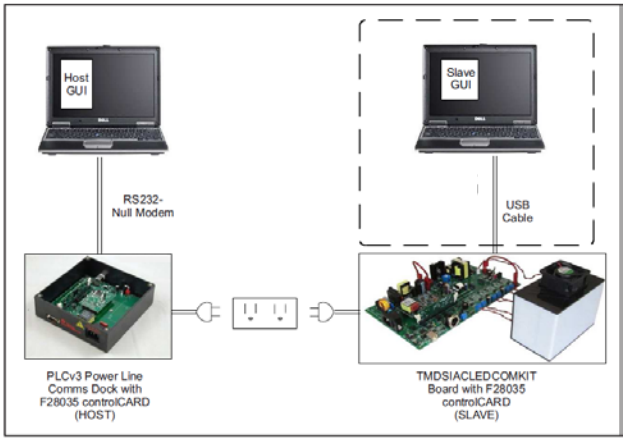

Figure 9: The experimental environment of real power-line channel.

Before the communication starts, we measured the channel noise by the receiver. Both frequency and time domain match the multipath model in Eq. (7).

The fidelity of the reconstructed image is measured with the Peak Signal-to-Noise Ratio (PSNR). It is the ratio between the maximum possible power of a signal and the power of corrupting noise that affects the fidelity of this signal. Because many signals have a very wide dynamic range, PSNR is usually expressed in terms of the logarithmic decibel scale. The PSNR is defined as follows [29]:

$$PSNR = 10\log_{10}\left(\frac{\max_f^2}{MSE}\right) \tag{21}$$

where $\max_f$ is the maximum possible pixel value of an image *f*, for 8 bit pixels, $\max_f = 255$. *MSE* is the Mean Square Error. For an $N \times N$ monochrome image, it is defined as:

$$MSE = \frac{\sum\left[f(i,j) - \hat{f}(i,j)\right]^2}{N^2} \tag{22}$$

where $f(i,j)$ is the source image and $\hat{f}(i,j)$ is the reconstructed image.

Figures 10, 11 and 12 show a comparison between the received images at different SNR values using the presented real PLC system (DFT-based OFDM with bit interleaving), the conventional CPM-OFDM system (without interleaving) and the proposed CPM-based DCT-OFDM system with and without chaotic interleaving.

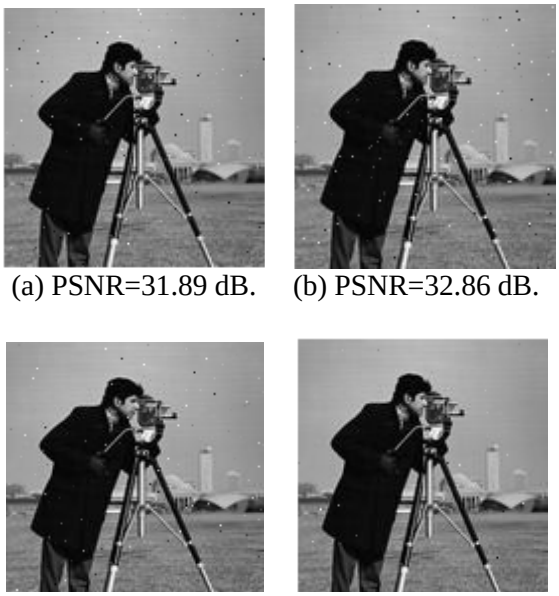

(a) PSNR=31.89 dB. (b) PSNR=32.86 dB.

(c) PSNR =35.68 dB. (d) PSNR=37.87 dB.

Figure 10: The received cameraman image using (a) real PLC system, (b) conventional CPM-OFDM system, (c) proposed CPM-based DCT-OFDM system without chaotic interleaving and (d) proposed CPM-based DCT-OFDM system with chaotic interleaving at SNR= 7.5 dB.

7 Conclusion

This paper proposed a new transceiver scheme to improve BPLC performance. The proposed transceiver is implemented by CPM-based DCT-OFDM system. This paper also presented a chaotic interleaving scheme for the proposed transceiver to further improve the BER performance of BPLC. Computer simulations and real-life experiment were used to evaluate the proposed transceiver. It was shown that, the proposed transceiver scheme was robust to channel impairments while maintaining superior BER performance especially when using chaotic interleaving. As a real application of PLC, we check the transmissions of cameraman image over a real PLC channel. Images with high PSNR were received and the proposed transceiver was shown to have a good performance over BPLC channels.

(a) PSNR=34.03 dB. (b) PSNR =36.68 dB.

(c) PSNR=39.47 dB. (d) PSNR=43.37 dB.

Figure 11: The received cameraman image using (a) real PLC system, (b) conventional CPM-OFDM system, (c) proposed CPM-based DCT-OFDM system without chaotic interleaving and (d) proposed CPM-based DCT-OFDM system with chaotic interleaving at SNR= 10 dB.

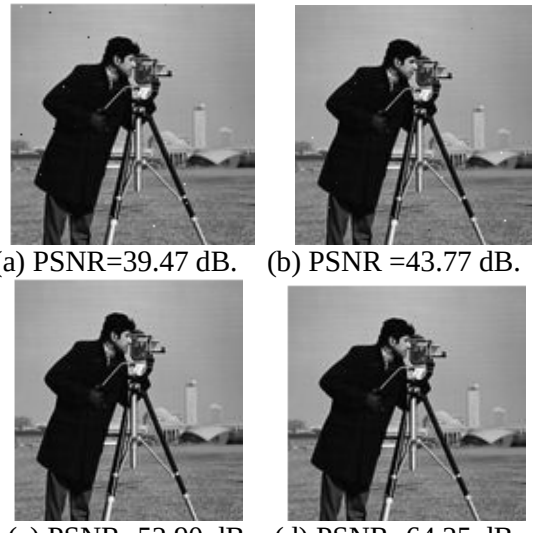

(a) PSNR=39.47 dB. (b) PSNR =43.77 dB.

(c) PSNR=52.90 dB. (d) PSNR=64.25 dB.

Figure 12: The received cameraman image using (a) real PLC system, (b) conventional CPM-OFDM system, (c) proposed CPM-based DCT-OFDM system without chaotic interleaving and (d) proposed CPM-based DCT-OFDM system with chaotic interleaving at SNR= 12.5 dB.

Acknowledgement

The authors would like to express their gratitude to Deanship of Scientific Research (SABIC 2), Jazan University, Jazan, Saudi Arabia for supporting this work.

References

[1] K. Dostert, "Power line Communications", Prentice-Hall, NJ, 2001.

[2] X. Carcelle, "Power Line Communications in Practice", Artech House, London, 2006.

[3] G. Held, "Understanding Broadband over Power Line", Auerbach Publications, New York, 2001.

[4] H. C. Ferreira, L. Lampe, J. Newbury and T. G. Swart, "Power Line Communications: Theory and applications for narrowband and broadband communications over power lines", John Wiley & Sons, 2006.

[5] M. Zimmermann and K. Dostert, "A multipath model for the power line channel," IEEE Transactions on Communications, vol. 50, no. 4, pp. 553-559, Apr. 2002.

[6] M. Götz, M. Rapp and K. Dostert, "Power line channel characteristics and their effect on communication systems design", *IEEE Commun. Magazine*, Vol. 42, No. 4, pp. 78-86, Apr. 2004.

[7] M. Zimmermann and K. Dostert, "Analysis and modeling of impulsive noise in broad-band power line communications," IEEE Transactions on Electromagnetic Compatibility, vol. 44, no. 1, pp. 249-258, Feb. 2002.

[8] H. Meng, Y. L. Guan and S. Chen, "Modeling and analysis of noise effects on broadband power-line communications", *IEEE Trans. Power Delivery.*, Vol. 20, No. 2, pp. 630-637, Apr. 2005.

[9] S. Tseng, Y. Hsu, Y. Peng," Iterative multicarrier detector and LDPC decoder for OFDM systems," WSEAS Trans. on Commun., vol. 11, pp. 124-134, March 2012.

[10] R. V. Nee and R. Prasad, OFDM for Wireless Multimedia Communications, Artech House, 2000.

[11] S. B. Weinstein, "The history of orthogonal frequency division multiplexing," IEEE Commun. Mag., pp. 26-35, Nov. 2009.

[12] E. S. Hassan, Xu Zhu, S.E. El-Khamy, M.I. Dessouky, S.A. El-Dolil, F.E. Abd El-Samie, "Performance Evaluation of OFDM and Single-Carrier Systems Using Frequency Domain Equalization and Phase Modulation", Int. J. Commun. Syst., vol. 24, pp.1–13, 2011.

[13] E. S. Hassan, Xu Zhu, S.E. El-Khamy, M.I. Dessouky, S.A. El-Dolil, F.E. Abd El-Samie, "Enhanced performance of OFDM and single-carrier systems using frequency domain equalization and phase modulation", Proc. of NRSC-09, Egypt, March 17-19, 2009.

[14] N. Moret and A. M. Tonello, "Performance of filter bank modulation with phase noise," *IEEE Trans. Wireless Commun*., vol. 10, no. 10, pp. 3121–3126, Oct. 2011.

[15] N. Al-Dhahir and H. Minn, "A new multicarrier transceiver based on the discrete cosine transform," in Proc. IEEE Wireless Commun. Netw. Conf., New Orleans, LA Mar. 2005, pp. 45–50.

[16] G. D. Mandyam, "Sinusoidal Transforms in OFDM System," *IEEE Trans. On Broadcasting*. vol. 50, no. 2, June 2004, pp. 172-184.

[17] F. Cruz-Rold´an, M. Elena, G. Vidal, J. Ave, and M. Velasco, "Single-Carrier and Multicarrier Transceivers Based on Discrete Cosine Transform Type-IV," IEEE Trans. Wireless Commun., vol. 12, no. 12, pp. 6454–6463, Dec. 2011.

[18] P. Tan, and N. C. Beaulieu, "A Comparison of DCT-Based OFDM and DFT-Based OFDM in Frequency Offset and Fading Channels," IEEE *Trans. On Commun*., vol. 54, no. 11, Nov. 2006, pp. 2113-2125.

[19] E.S. Hassan, Xu Zhu, S.E. El-Khamy, M.I. Dessouky, S.A. El-Dolil, F.E. Abd El-Samie, "A Continuous Phase Modulation Single-Carrier Wireless System with Frequency Domain Equalization", Proc. of the IEEE International Conference on Computer Engineering and systems (ICCES'09), Cairo, Egypt, 14–16 Dec. 2009.

[20] E. S. Hassan, "Performance Enhancement of Continuous-Phase Modulation Based OFDM Systems Using Chaotic Interleaving", WSEAS Transactions on Systems, vol. 12, no. 1, pp. 1-10, Jan. 2013.

[21] E. S. Hassan, Xu Zhu, S.E. El-Khamy, M.I. Dessouky, S.A. El-Dolil, F.E. Abd El-Samie, "Chaotic interleaving scheme for single-and multi-carrier modulation techniques implementing continuous phase modulation," *Journal of the Franklin Institute*, vol. 350, no. 4, pp. 770–789, May 2013.

[22] E.S. Hassan, Xu Zhu, S.E. El-Khamy, M.I. Dessouky, S.A. El-Dolil, F.E. Abd El-Samie, "New Interleaving Scheme for Continuous Phase Modulation Based OFDM Systems Using Chaotic Maps", *Proc. of the IEEE International Conference on Wireless and Optical Communications Networks* (WOCN-09), Cairo, Egypt, 28–30 April, 2009.

[23] E. S. Hassan, Xu Zhu, S.E. El-Khamy, M.I. Dessouky, S.A. El-Dolil, F.E. Abd El-Samie, "A Chaotic Interleaving Scheme for Continuous Phase Modulation Based Single-Carrier Frequency-Domain Equalization Systems", *Wireless Personal Commu.*, vol. 62, no. 1, pp.183-199, Jan., 2012.

[24] R. Pighi, M. Fraceschini, G. Ferrari and R. Raheli, "Fundamental performance limits of communications systems impaired by impulsive noise", *IEEE Trans. Commun.*, Vol. 57, No. 1, pp. 171-182, Jan. 2009.

[25] Y. H. Ma, P. L. So and E.Gunawan, "Performance analysis of OFDM systems for broadband power line communications under impulsive noise and multipath", *IEEE Trans. Power Delivery*, Vol. 20, No. 2, pp. 674-681, Apr. 2005.

[26] F. Han, X. Yu, and S. Han, "Improved baker map for image encryption," in *ISSCAA*, 2006, pp. 1273–1276.

[27] http://www.ti.com/tool/TIDM-TMDSPLCKIT-V3, last access 21-3-2015.

[28] http://www.ti.com/tool/tmdsiacledcomkit?DCMP=piccolo-led&HQS=piccolo-led-b, last access 21-3-2015.

[29] E. M. El-Bakary, E. S. Hassan, O. Zahran, S. A. El-Dolil, and F. E. Abd El-Samie "Efficient image transmission with multi-carrier CDMA", *Wireless Personal Commu*., DOI 10.1007/s11277-012-0622-6. 2012.